



Published in final edited form as:

J Neuroimmune Pharmacol. 2018 March ; 13(1): 64–76. doi:10.1007/s11481-017-9761-6.

Differential Effects of Antiretroviral Drugs on Neurons In Vitro: Roles for Oxidative Stress and Integrated Stress Response

Anna L. Stern¹, Rebecca N. Lee¹, Nina Panvelker¹, Jiean Li¹, Jenna Harowitz¹, Kelly L. Jordan-Sciutto¹, and Cagla Akay-Espinoza¹

¹Department of Pathology, School of Dental Medicine, University of Pennsylvania, 240 S. 40th St. Rm. 312 Levy Building, Philadelphia, PA 19104-6030, USA

Abstract

Mounting evidence suggests that antiretroviral drugs may contribute to the persistence of HIV-associated neurocognitive disorders (HAND), which impact 30%–50% of HIV-infected patients in the post-antiretroviral era. We previously reported that two first generation HIV protease inhibitors, ritonavir and saquinavir, induced oxidative stress, with subsequent neuronal death in vitro, which was reversed by augmentation of the endogenous antioxidant response by monomethyl fumarate. We herein determined whether two newer-generation PIs, darunavir and lopinavir, were deleterious to neurons in vitro. Further, we expanded our assessment to include three integrase strand transfer inhibitors, raltegravir, dolutegravir, and elvitegravir. We found that only lopinavir and elvitegravir were neurotoxic to primary rat neuroglial cultures as determined by the loss of microtubule-associated protein 2 (MAP2). Intriguingly, lopinavir but not elvitegravir led to oxidative stress and induced the endogenous antioxidant response (EAR). Furthermore, neurotoxicity of lopinavir was blocked by pharmacological augmentation of the endogenous antioxidant heme oxygenase-1 (HO-1), expanding our previous finding that protease inhibitor-induced neurotoxicity was mediated by oxidative stress. Conversely, elvitegravir but not lopinavir led to increased eIF2 α phosphorylation, indicating the activation of a common adaptive pathway termed the integrated stress response (ISR), and elvitegravir-mediated neurotoxicity was partially alleviated by the ISR inhibitor trans-ISRIB, suggesting ISR as a promoter of elvitegravir-associated neurotoxicity. Overall, we found that neurotoxicity was induced only by a subset of protease inhibitors and integrase strand transfer inhibitors, providing evidence for class- and drug-specific neurotoxic effects of antiretroviral drugs. Future in vivo studies will be critical to confirm the neurotoxicity profiles of these drugs for incorporation of these findings into patient management. The EAR and ISR pathways are potential access points for the development of adjunctive therapies to complement antiretroviral therapies and limit their contribution to HAND persistence.

Correspondence to: Cagla Akay-Espinoza.

Compliance with Ethical Standards

Ethics Statement: All applicable international, national, and/or institutional guidelines for the care and use of animals were followed. All procedures performed in studies involving animals were in accordance with the ethical standards of the institution or practice at which the studies were conducted. This article does not contain any studies with human participants performed by any of the authors.

Keywords

HIV; HIV-associated neurocognitive disorders; Antiretroviral therapy; Heme oxygenase-1; Oxidative stress; Integrated stress response

Introduction

Human immunodeficiency virus (HIV) affects 36.9 million people globally (UNAIDS 2015) and 1.1 million people in the United States alone (Centers for Disease Control and Prevention 2016). Left untreated, HIV replicates in blood and tissues, eventually leading to debilitating loss of immune function defined as acquired immune deficiency syndrome (AIDS). AIDS patients are susceptible to opportunistic infections which are often lethal. However, the introduction of combination antiretroviral therapy in 1996 transformed HIV diagnosis from a death sentence into a chronic, manageable condition with minimal to no effect on life expectancy in the absence of comorbidities (Lai et al. 2006; Teeraananchai et al. 2016).

Despite the pronounced benefits of antiretroviral therapy, the incidence of neurological complications among HIV-infected individuals has not declined. In fact, HIV-associated neurocognitive disorders (HAND) remain prevalent, with estimates ranging between 15% and 55% in HIV-infected patients (Saylor et al. 2016). Although the diagnosis of severe neurological dysfunction, termed HIV-associated dementia (HAD), is now rare, the incidence of both asymptomatic neurocognitive impairment (ANI) and mild neurocognitive disorder (MND) has increased (Sacktor et al. 2016). Additionally, while approximately 70% of HAND patients are asymptomatic, ANI patients are two to six fold more likely than neurocognitively normal patients to progress to symptomatic disease (Grant et al. 2014). Moreover, with the expected increase in life expectancy of HIV-infected individuals afforded by antiretroviral therapy, age-related changes in the central nervous system (CNS) may exacerbate HAND symptoms (Gelman and Schuenke 2004; Cohen et al. 2015; Tan et al. 2013).

Persistence of HAND despite viral suppression by antiretroviral therapy is not well understood. The cause is likely multifactorial, with contributions from HIV-related factors (Kaul and Lipton 2006; Chen et al. 2014) as well as from antiretroviral drugs (ARVs) themselves (Treisman and Soudry 2016; Shah et al. 2016). Several studies found that ARVs with higher CNS penetration effectiveness were associated with more frequent neurological symptoms, indicating a role for ARV toxicity (Marra et al. 2009; Caniglia et al. 2014; but see Carvalhal et al. 2016; Smurzynski et al. 2011 for alternative results). Numerous studies also demonstrated the potential for ARVs to cause oxidative stress, endoplasmic reticulum (ER) stress, and mitochondrial dysfunction, with subsequent synaptodendritic damage and neuron loss both in vivo and in vitro (Akay et al. 2014; Gannon et al. 2017; Robertson et al. 2012; Brown et al. 2014). As neurotoxicities associated with different ARVs may vary, and given the continuing development of newer and more effective ARVs, questions remain regarding the potential for current therapies to instigate long-term adverse neurological effects.

ARVs can be broadly categorized into five classes according to their mechanism of action: entry inhibitors, nucleoside reverse transcriptase inhibitors (NRTIs), nonnucleoside reverse transcriptase inhibitors (NNRTIs), integrase strand transfer inhibitors (INSTIs), and protease inhibitors (PIs). Currently, the United States Department of Health and Human Services (DHHS) recommends that frontline treatment for adult HIV-infected individuals should include either an INSTI or a PI in combination with two NRTIs (DHHS 2016a). We previously showed that two first generation PIs, ritonavir and saquinavir, led to oxidative stress and neurotoxicity (Akay et al. 2014). Herein, we expanded our investigation to include three INSTIs, elvitegravir (EVG), dolutegravir (DTG), and raltegravir (RAL), as well as two commonly used PIs darunavir (DRV) and lopinavir (LPV). All are currently recommended by the DHHS as frontline treatment options for adults and adolescents, except for LPV which is recommended by the DHHS and the WHO for all children under three years of age (DHHS 2016a; WHO 2016a). We investigated the neurotoxicity profiles of these ARVs in vitro and examined the underlying mechanisms contributing to toxicity.

Materials and Methods

Chemicals and Reagents

The following antibodies were purchased from the indicated vendors: Enzo Life Sciences (Farmingdale, NY): heme oxygenase-1 (HO-1, ADI-SPA-896); Abcam (Cambridge, MA): glutathione-S-reductase (GSR, ab16801); Cell Signaling Technology (Danvers, MA): phosphorylated eukaryotic initiation factor 2 α (peIF2 α , 9721), total eIF2 α (9722); BD Transduction Laboratories (San Jose, CA): binding immunoglobulin protein (BiP, 610,978); BioLegend (San Diego, CA): microtubule-associated protein 2 (MAPs2, 801,801). The following chemical reagents were purchased from the indicated vendors: Citifluor (London, UK): 4',6-diamidino-2-phenylindole (DAPI); Invitrogen (Carlsbad, CA): Dulbecco's Modified Eagle's Medium (DMEM), neurobasal medium, B27 supplement; BioRad (Hercules, CA): Bradford protein assay dye, polyvinylidene fluoride (PVDF) membrane, prestained broad range molecular weight ladder; Sigma Aldrich (St. Louis, MO): Tween 20, Triton X-100, Fast Green FCF, protease inhibitor cocktail, bovine serum albumin (BSA), dimethyl sulfoxide (DMSO); Peptides International (Louisville, KY): Poly-L-Lysine; Scytek Labs (Logan, UT): normal antibody diluent (NAD); Millipore (Temecula, CA): Luminata Classico ECL; Thermo Fisher Scientific (Waltham, MA): CellRox Green, tetramethylrhodamine methyl ester (TMRM); Tocris Bioscience (Bristol, UK): 1-(2-Cyano-3,12,28-trioxooleana-1,9(11)-dien-28-yl)-1H-imidazole (CDDO), *N,N'*-*trans*-1,4-cyclohexanediylbis[2-(4-chlorophenoxy)acetamide] (*trans*-ISRIB). All horse radish peroxidase (HRP)-conjugated secondary antibodies were obtained from Thermo Fisher Scientific, and all fluorescent dye-conjugated secondary antibodies were obtained from Jackson ImmunoResearch Labs (West Grove, PA). ARVs were kindly provided by the AIDS Research and Reference Reagent Program, Division of AIDS, National Institute of Allergy and Infectious Diseases, NIH (Bethesda, MD).

Preparation of Primary rat Cortical Neuroglial Cultures

Primary rat cortical cultures were prepared from embryonic day 18 Sprague-Dawley rat embryos (Charles River Laboratories, Seattle, WA). Brains were isolated, and dissected

cortices were incubated for 40 min in DMEM +0.027% trypsin as described previously (Wilcox et al. 1994). Cells were then washed in saline, triturated, resuspended in neurobasal media supplemented with B27, and plated on poly-L-lysine-coated 6-well (9.4-cm² growth area) or 24-well (1.9-cm² growth area) plates (USA Scientific, Ocala, FL) at a concentration of 500,000 cells/ml. Cultures contained approximately 90% neurons and 10% astrocytes/glia and were maintained in neurobasal media supplemented with B27 at 37 °C with 5% CO₂ as described previously (Gannon et al. 2017; Akay et al. 2011). On 10 days in vitro (DIV), 20% fresh media was added. Cells were treated on DIV 14–16.

Drug Treatments

Cells were treated with individual ARVs for the times and doses as indicated. DTG, RAL, and EVG were prepared as 50-mM stock solutions in DMSO, whereas RTV, LPV, and DRV were prepared as 25-mM stock solutions in DMSO. In specific experiments, CDDO (prepared as a 50-mM stock solution in DMSO) or trans-ISRIB (prepared as a 10-mM stock solution in DMSO) was used for 1-h pretreatment before the indicated ARV treatments.

Immunofluorescence

Following treatment, cells were rinsed with phosphate-buffered saline (PBS) and fixed with 4% paraformaldehyde for 20 min. Cells were then rinsed twice in PBS and three times in PBS containing 0.1% Tween 20 (PBS-T), followed by a 30-min incubation with a blocking/permeabilization solution containing 0.2% BSA + 0.1% Triton-X in PBS. Cells were rinsed three times in PBS-T and incubated with MAP2 primary antibody diluted at 1:4000 in NAD for 2 h at room temperature. Following three washes in PBS-T, cells were then incubated with a FITC-conjugated goat anti-mouse secondary antibody diluted at 1:500 in NAD for 30 min at room temperature. Cells were then imaged using a Keyence BZ-X-700 digital fluorescent microscope (Keyence Corporation, Itasca, IL) affixed with UV, FITC, Cy3, and Cy5 filters. Images captured at ×20 magnification were analyzed with the BZ-X Keyence software to quantify the number of neurons. Specifically, the number of neurons, identified as cells expressing MAP2, was averaged across a total of 25 fields/well, with 2–4 wells/treatment condition for each biological replicate. Data were analyzed using GraphPad Prism statistical software (version 7.0; GraphPad, San Diego, CA), and data were expressed as mean fold change from untreated (UT) ± standard error of the mean (SEM).

Immunoblotting

Following treatment, cells were rinsed twice with PBS and lysed with whole cell lysis buffer (50 mM Tris pH 7.5, 120 mM NaCl, 0.5% NP-40, 0.4 mM NaF, 0.4 mM Na₃VO₄, and 1:100 protease inhibitor cocktail). Protein supernatants were collected with centrifugation at 20,000 *g* for 10 min at 4 °C. Protein concentrations were determined using the Bradford method, and 3–5 µg total protein per condition was loaded into each lane of precast 10% Bis-Tris NuPAGE Novex gels (Thermo Fisher Scientific). Proteins were then transferred to PVDF membranes, which were blocked with 5% BSA in tris-buffered saline containing 0.1% Tween 20 (TBS-T) for 1 h at room temperature and incubated overnight with primary antibodies at 4 °C. Following three washes in TBS-T, membranes were incubated with HRP-conjugated secondary antibody (1:5000 in 5% BSA + TBS-T) for 30 min at room temperature. Bands were visualized by chemiluminescence with Luminata Classico ECL,

and images were captured by film development or ChemiDoc Touch imaging system (BioRad). Equal loading and even transfer of samples were confirmed using fast green staining of the membranes. Densitometric analysis of band intensities was conducted using ImageJ software (v1.44, NIH), and all bands were normalized to fast green stain. Data were analyzed using GraphPad Prism statistical software, and data were expressed as mean fold change from UT \pm SEM.

CellRox Green Live Cell Imaging

CellRox Green oxidative stress detection reagent was purchased as a stable 2.5-mM solution dissolved in DMSO. Aliquots were stored at -20°C protected from light and with a desiccant, thawed just prior to use. Directly following drug treatments, CellRox was added to cell media at a final concentration of $5\ \mu\text{M}$ and incubated at 37°C for 30 min according to manufacturer's instructions. Cells were then visualized at $20\times$ using Keyence BZ-X-700 digital fluorescent microscope by time-lapse live cell imaging. Images of each well were captured approximately every 6 min for 1 h following the incubation period. Cell media were then removed, and cells were rinsed and fixed with 4% paraformaldehyde for 20 min prior to immunofluorescence staining, as described above. Images of cells stained with MAP2/DAPI were then merged with CellRox Green images using Adobe Photoshop. Quantification of CellRox Green fluorescence was achieved using Keyence BZ-X analysis software. Data were analyzed using GraphPad Prism statistical software, and data were expressed as mean fold change from UT \pm SEM.

Results

Elvitegravir but Not Dolutegravir or Raltegravir is Toxic to Neurons In Vitro

Given that INSTIs are an integral part of the updated frontline treatment for HIV, we first determined the effects of three commonly prescribed INSTIs, EVG, DTG, and RAL, on MAP2 expression in primary neuroglial cultures. We treated cells with individual ARVs at 0.1, 1, or $10\ \mu\text{M}$ either one time for two days or every other day for four days (see Table 1 for comparison with in vivo concentrations of INSTIs used in this study). While 2- and 4-day treatments with EVG at lower concentrations did not lead to neuronal damage as determined by the reduction in the number of MAP2-positive cells, $10\ \mu\text{M}$ EVG led to a nonsignificant decrease in MAP2 at 2 days and an average of 76% MAP2 loss at 4 days (Fig. 1a, b). In contrast, neither DTG (Fig. 1a, c) nor RAL (Fig. 1a, d) was neurotoxic at any dose or time point tested.

Lopinavir but Not Darunavir is Toxic to Neurons In Vitro

PIs are the second most commonly prescribed ARVs. Specifically, DRV is the only currently recommended frontline PI for adults in the United States, whereas LPV is the PI of choice both in the United States and globally for the treatment of children under the age of three (DHHS 2016a; WHO 2016a). Hence, we determined the effects of these drugs on MAP2 expression in primary neuroglial cultures. We treated cells with ARVs individually at either 0.1, 1, or $10\ \mu\text{M}$ for 2 days (see Table 1 for comparison with in vivo measured concentrations of PIs used in this study). At lower concentrations, LPV was not toxic; however, $10\ \mu\text{M}$ LPV led to an average of 54% MAP2 loss (Fig. 2a, b). In contrast, DRV

was not toxic at any dose after 2 days. Surprisingly, treatment with 0.1 μM DRV led to an increase in the number of MAP2+ cells compared with the vehicle control (Fig. 2a, c).

In clinical practice, PIs are often administered with a low “booster” dose of RTV to inhibit the metabolism of concomitantly prescribed ARVs and increase their bioavailability. These combinations are packaged into fixed-ratio pill forms such that RTV dose is increased by the same ratio as the primary PI if the regimen is altered. Based on our previous work demonstrating that RTV was neurotoxic at 10 μM in vitro (Gannon et al. 2017; Akay et al. 2014), we determined whether lower doses of RTV administered as part of an ARV regimen could alter the effects of other PIs. Cells were treated for 2 days with LPV or DRV at 0.1, 1, or 10 μM concentrations either alone or with corresponding RTV booster concentrations of 0.02, 0.2, or 2 μM , respectively. Although 2 μM RTV was neurotoxic after two days regardless of concomitant treatment with DRV, none of the combinations tested were more toxic than either ARV alone (Fig. 2d).

Lopinavir but Not Elvitegravir Increases Reactive Oxygen Species (ROS)

We previously observed that ARVs caused oxidative stress in the CNS in vivo (Akay et al. 2014). Therefore, we next determined whether LPV and EVG led to ROS accumulation in neurons. The oxidative stress indicator CellRox Green was added to the culture media together with LPV or EVG, and live cell imaging was conducted 1 h later as described in the Methods section. The green fluorescence in the nucleus, indicating the accumulation of the oxidized compound in the presence of ROS, was significantly increased by LPV compared to DMSO vehicle control. In contrast to LPV, however, EVG did not lead to an increase in ROS; instead, both DMSO and EVG led to a reduction in ROS levels even below those measured in untreated cultures (Fig. 3a, b).

Lopinavir but Not Elvitegravir Activates the Endogenous Antioxidant Response

Based on our observation of oxidative stress induced by LPV, we sought to determine whether the endogenous antioxidant response was activated. To that end, we assessed the levels of heme oxygenase-1 (HO-1), a canonical indicator of endogenous antioxidant response activation with potent antioxidant properties, in lysates prepared from cultures treated with 0.1, 1, or 10 μM LPV for 4, 8, or 20 h. As shown in Fig. 4a and b, we observed that HO-1 protein levels were increased in cultures treated with 10 μM LPV for 20 h, in addition to a nonsignificant increase after 8 h. In contrast, EVG treatment had no significant effect on HO-1 (Fig. 4e, f). Another common mediator of cellular toxicity is an adaptive cellular response called the integrated stress response (ISR), which we previously identified as a correlate of neuropathological changes in HIV-infected patients (Lindl et al. 2007; Akay et al. 2012). Thus, we determined whether two canonical ISR markers, BiP and phospho-eIF2 α (peIF2 α), were altered in neurons exposed to 10 μM LPV or EVG for 4, 8, or 20 h. Surprisingly, we observed no changes in either BiP or the ratio of peIF2 α /teIF2 α following LPV treatment, aside from a nonsignificant increase in BiP after 20 h (Fig. 4a, c, d). In contrast, 10 μM EVG treatment led to an early increase in peIF2 α /teIF2 α at 4 h, followed by a decrease at 20 h (Fig. 4e, h).

Induction of Heme Oxygenase-1 by CDDO is Protective against Lopinavir-Induced Neurotoxicity

HO-1 is a critical endogenous antioxidant component of the cell, and its pharmacological induction was previously demonstrated to be protective against a variety of CNS insults including RTV-mediated neurotoxicity (Chen 2014; Cross et al. 2011; Akay et al. 2014). Thus, we hypothesized that augmentation of HO-1 might be neuroprotective against LPV-induced neuronal death. CDDO is a triterpenoid known to induce the expression of antioxidant response element genes including *HO-1* via activation of the transcription factor nuclear factor erythroid 2-related factor 2 (Nrf2) (Yates et al. 2007). We determined whether CDDO could augment HO-1 expression in LPV-treated cultures. Indeed, after 20 h of treatment, HO-1 was increased in cultures exposed to CDDO or LPV alone and was further increased by the combination of both compounds (Fig. 5a, b). Surprisingly, under the same conditions, neither CDDO nor LPV led to a change in the protein levels of glutathione reductase (GSR), another component of the endogenous antioxidant response targeted by Nrf2 (Fig. 5a, c). In agreement with its ability to augment HO-1 expression, CDDO pretreatment was able to completely block LPV-induced neurotoxicity (Fig. 5d, e), indicating both a mechanistic role for oxidative stress in LPV-mediated neurotoxicity as well as a neuroprotective role for HO-1. In contrast, consistent with our observed lack of ROS accumulation and HO-1 induction following EVG treatment, CDDO had no effect on EVG-induced neurotoxicity (Fig. 5f).

Attenuation of the Activation of Integrated Stress Response is Partially Protective against Elvitegravir-Induced Neurotoxicity

ISR is a common pathway activated for cellular adaptation to extrinsic factors (e.g. amino acid and/or glucose deprivation, viral infection, hypoxia) as well as intrinsic stress pathways (e.g. ER stress); eIF2 α phosphorylation plays a central role in ISR in a wide variety of physiological and pathological conditions including numerous neurodegenerative diseases, as evidenced by neuroprotection achieved with the inhibition of eIF2 α phosphorylation (Halliday and Mallucci 2014; Hetz and Mollereau 2014; Halliday et al. 2015). Therefore, we determined whether reducing eIF2 α phosphorylation was neuroprotective against EVG-induced neuronal death. A small molecule, trans-ISRIB, was recently shown to prevent peIF2 α -mediated ISR activation and improve memory in vivo (Sidrauski et al. 2013). We determined whether trans-ISRIB could attenuate the EVG-mediated increase in peIF2 α and subsequent neurotoxicity. As shown in Fig. 6a, 1-h pretreatment with trans-ISRIB led to a reduction in peIF2 α in EVG-treated neurons, whereas total eIF2 α levels were not affected by trans-ISRIB treatment. Furthermore, EVG-induced neurotoxicity was significantly attenuated in cultures that were pretreated with trans-ISRIB (Fig. 6b, c), suggesting ISR as a contributor in EVG-mediated neurotoxicity and trans-ISRIB as a potential neuroprotective agent.

Discussion

The introduction of ART was a life-saving advancement in HIV/AIDS, and our most urgent goal is to expand access to therapy around the world (WHO 2016b). However, given the continued persistence of HAND despite effective viral suppression with ARVs, a better

understanding of potential ARV neurotoxicities is necessary as patients remain on ART for decades due to increased lifespan. In particular, the most recently introduced class of ARV, INSTIs, requires further investigation as their worldwide use continues to grow.

In the present study, we investigated the *in vitro* effects of five drugs including the INSTIs EVG, DTG, and RAL and the PIs LPV and DRV, all of which are recommended as part of current frontline regimens for HIV-infected individuals in the U.S (DHHS 2016a; DHHS 2016b). Neuronal damage was induced by EVG and LPV only, and LPV but not EVG led to oxidative stress while EVG but not LPV led to transient ER stress. Furthermore, pharmacological induction of the endogenous antioxidant HO-1 was sufficient to reverse LPV-induced neuronal damage, and attenuation of the ISR by trans-ISRIB partially protected against EVG-induced neuronal damage.

Of the three INSTIs tested, only EVG caused neuronal damage in primary rat cultures. This within-class difference was dramatic, with EVG causing a 76% loss of MAP2, whereas the same dose and time course of treatment with DTG or RAL had no effect. Of note, DRV actually led to an increase in the number of MAP2+ cells after 2-day treatment with the lowest dose, which may represent a protective effect against minor neurotoxicity of the DMSO vehicle. These data also corroborate previous studies showing the lack of *in vitro* toxicity of RAL (Blas-Garcia et al. 2014). Thus, it may be warranted for clinicians to consider this observation when deciding between the three drugs, especially in younger patients who are anticipated to take ARVs for several decades. However, it is critical to interpret these data with caution and in the full context of other studies. For instance, while we found no evidence of neurotoxicity with DTG in our model, which was consistent with many comprehensive studies of patient populations (Kanters et al. 2016; Singh et al. 2016a), other recent evidence indicates that potential CNS toxicity of DTG should not be overlooked (Hoffmann et al. 2017; Kheloufi et al. 2015; de Boer et al. 2016). Neuropsychiatric side effects of DTG might be due to its relatively high CNS penetration effectiveness, with CSF concentrations reaching levels equivalent to those measured in plasma (Letendre et al. 2014). Moreover, many ARVs as well as their metabolites can have severe peripheral side effects including chronic inflammation (Troya and Bascuñana 2016), which may indirectly cause neuropsychiatric symptoms.

Additionally, we found a difference in the neurotoxic potential of two PIs, DRV and LPV. Specifically, LPV caused a 54% loss of MAP2, whereas DRV had no effect at the same dose and time course. The relevance of this direct comparison is highlighted by comparable recommended dosing and maximum plasma concentrations of the two drugs in patients (see Table 1). Moreover, DRV had no effect on neurons even when combined with low doses of RTV, as it is currently prescribed. Future studies should address whether combinations of DRV and cobicistat, the newest approved co-formulation, remain non-neurotoxic (Capetti et al. 2015). These results add to a growing body of *in vitro* evidence that DRV is a particularly safe treatment option (Robertson et al. 2012; Blas-Garcia et al. 2014). DRV was designed to bind tightly to the HIV protease and limit drug resistance (Deeks 2014; Wensing et al. 2010); moreover, DRV demonstrated superior viral suppression, increased CD4⁺ T cell counts, and a lower incidence of gastrointestinal side effects in a direct comparison study with LPV (Mills et al. 2009). Despite these data, LPV is prescribed more frequently than

DRV in resource-poor areas, such as Sub-Saharan Africa where over 70% of HIV-infected individuals reside (Saylor et al. 2016; WHO 2016a). The prevalence of LPV use in resource-poor settings is primarily because LPV is available as a generic, heat stable fixed-dose combination drug approved for once-daily dosing (WHO 2016a). Our study along with those mentioned above highlight the rationale for urgent development of a similar formulation of DRV available at lower cost.

Another relevant consideration is that LPV is recommended by the DHHS (2016b) and WHO (2016a) as the frontline treatment for newborns and children up to three years of age. In addition to the evidence of blood brain barrier disruption caused by HIV in general (Singh et al. 2016b; Nakagawa et al. 2012; Singh et al. 2014), data suggest that the blood brain barrier in newborns is not yet fully developed (Baburamani et al. 2012; Watson et al. 2006; but see Saunders et al. 2012 for an alternative view), which raises the possibility that infant brains might be exposed to higher concentrations of ARVs than adults. This consideration highlights the need for future studies on LPV and its effects on neurons *in vivo*, particularly in models of pediatric infection.

In addition to characterizing the effects of LPV and EVG on neuronal damage indicated by MAP2 expression, we investigated several mechanisms that might be involved. We expected to observe activation of the ISR, given previous reports by us and others showing the potential for PIs to activate the ISR pathway *in vivo* and *in vitro* (Gannon et al. 2017; De Gassart et al. 2016; Weiß et al. 2016; Borsa et al. 2015). Interestingly, LPV did not upregulate ISR markers BiP or peIF2 α , indicating that the mechanism driving neurotoxicity might be distinct from that of other PIs (Gannon et al. 2017). However, a lack of effect on BiP and peIF2 α does not rule out the possibility that LPV induces ISR. These indicators only represent one arm of the ISR, and other elements of the ISR may be preferentially induced in response to LPV. In contrast to LPV, EVG treatment transiently increased the ratio of peIF2 α /teIF2 α , indicating potential ISR activation. This increase was no longer observed after 8 h treatment, which may reflect the ability of neurons to recover. This recovery is consistent with the observation that a single EVG treatment had no effect on MAP2 after 2 days.

LPV treatment led to oxidative stress, as evidenced by both increased ROS production and activation of the endogenous antioxidant response. These data are consistent with observations of ARV-associated mitochondrial dysfunction (Noguera-Julian et al. 2015) as well as our previous data linking ARVs to oxidative stress (Akay et al. 2014). Specifically, we found that two first-generation PIs, RTV and saquinavir, led to ROS accumulation in cultured neurons and that the neurotoxicity induced by these ARVs was blocked by augmenting the endogenous antioxidant response to reduce oxidative stress. In agreement with these observations, we herein again showed a mechanistic role for oxidative stress in ARV-induced neuronal damage, as LPV-induced damage was reversed by pharmacological induction of the endogenous antioxidant HO-1. Interestingly, both LPV and CDDO selectively induced HO-1 but not the additional Nrf2 target GSR. In previous studies, CDDO induced the canonical Nrf2 signaling pathway and increased GSR under certain conditions (Lu et al. 2016). The possibility remains that GSR was indeed increased in our experiments as well but that the rapid oxidation of GSR restored the enzyme to normal levels prior to our

earliest time point. A second possibility is that subcellular localization of HO-1, which, unlike GSR, is typically anchored to the ER (Schuller et al. 1998), may have played a role. Indeed, if increased ROS resulted in changes in ER calcium stores, this would preferentially affect HO-1 levels (Linden et al. 1998). Importantly, neuroprotection afforded by HO-1 is not always related to Nrf2. In one study, the compound gartanin prevented neuronal damage induced by glutamate through Nrf-2-independent mechanisms involving HO-1 (Gao et al. 2016), indicating that HO-1 can be independently implicated in neuroprotection without engagement of the endogenous antioxidant response in its entirety.

Further demonstrating the distinct mechanisms of toxicity across different ARVs, neither oxidative stress, HO-1 induction, nor protective potential of CDDO was observed with EVG treatment. In contrast to our findings regarding LPV, EVG treatment led to an early increase in the ratio of p $\text{eIF}2\alpha$ / $\text{tEIF}2\alpha$, indicating ISR activation. Moreover, the ISR inhibitor trans-ISRIB mediated partial neuroprotection in cultures exposed to EVG for 4 days, together with a reduction in p $\text{eIF}2\alpha$ levels after 4 h treatment, providing further evidence for ISR activation as a contributor to EVG-mediated neuronal damage in our in vitro model. The resolution of p $\text{eIF}2\alpha$ increase by 8 h after EVG treatment and the observation that a single EVG treatment had no effect on MAP2 after 2 days may reflect the ability of neurons to recover following acute exposure. Prolonged EVG exposure, however, may overwhelm the cellular capacity to resolve ISR activation. Importantly, our combined observations regarding LPV and EVG highlight critical differences in the neurotoxic potential and underlying neurotoxic mechanisms across ARV classes as well as within each class.

One important caution in the interpretation of our data is that these studies were done in vitro, and cultured neurons may not respond to ARVs in a similar manner as neurons in vivo, even within the same species. Moreover, there may be species differences, which indicates a need for further studies on these drugs in additional rodent strains, non-human primates, and humans. Relatedly, these studies did not identify the role of neuron-glia interaction in both the toxic and protective effects observed. Because the experiments were performed in neuroglial cultures, potential contributions of astrocytes and microglia should not be overlooked. Another legitimate concern about the relevance of our findings is whether the doses at which neurotoxic effects were observed were comparable to those expected in patients. Doses tested in the current study were designed to cover a wide range of concentrations, and the concentrations which caused neuronal damage in our in vitro system were 333-fold and 83-fold higher than those observed in patient CSF samples for EVG and LPV, respectively (Table 1). Hence, one important outcome of our study was that acute administrations of the five ARVs tested were not neurotoxic in vitro at low doses comparable to their reported concentrations in the CSF. However, although low doses had no effect on cell number quantified by MAP2+ cell counts, the possibility of synaptic damage remains, consistent with our previous studies (Akay et al. 2014). Additionally, a critical feature of our model is its attempt to assess the chronic effects of ART over decades utilizing an acute model, which necessitates higher drug concentrations than may be observed in the CSF of patients at any given time. Moreover, CSF drug concentrations may not accurately reflect ARV concentrations in the brain parenchyma (Anthonypillai et al. 2004). Finally, as current attempts are focused on improving the CNS penetration effectiveness of ARVs to

increase viral suppression in the brain (Bertrand et al. 2016), an understanding of the neurotoxic potential of even relatively high drug concentrations remains important.

In summary, the significance of the present study is twofold. First, we demonstrated that certain ARVs may have significant neurotoxic potential, which should influence the momentum for further in vivo studies of ARVs that ultimately aim to increase global access to ARVs with the highest safety indications. Second, we showed that ARVs caused neurotoxicity through distinct cellular pathways even within a single drug class. As adjunctive therapies are developed in attempts to treat the symptoms of HAND, it may be prudent to individualize therapies and include strategies to protect patients based on their specific ARV regimens.

Acknowledgments

We thank Margaret Maronski for her help in the preparation of primary rat cortical neuroglial cultures, Ping Lin for her technical assistance, the NIH AIDS reagent program for their generous donation of ARVs, and Dr. Sarah Ratcliffe for her help with statistical analysis.

Funding

We thank the NIH for the following funding sources: R01MH109382, R01MH106967, R01MH098742 (K.J-S). The following reagents were obtained through the AIDS Reagent Program, Division of AIDS, NIAID, NIH: lopinavir, darunavir, and raltegravir.

Grant Support: Financial support was provided by NIH grants MH098742, MH106967, and MH109382.

References

- Akay C, Lindl KA, Wang Y, White MG, Isaacman-Beck J, Kolson DL, Jordan-Sciutto KL. Site-specific hyperphosphorylation of pRb in HIV-induced neurotoxicity. *Mol Cell Neurosci*. 2011; 47:154–165. [PubMed: 21504794]
- Akay C, Lindl KA, Shyam N, Nabet B, Goenaga-Vazquez Y, Ruzbarsky J, Wang Y, Kolson DL, Jordan-Sciutto KL. Activation status of integrated stress response pathways in neurons and astrocytes of HIV-associated neurocognitive disorders (HAND) cortex. *Neuropathol Appl Neurobiol*. 2012; 38:175–200. [PubMed: 21883374]
- Akay C, Cooper M, Odeleye A, Jensen BK, White MG, Vassoler F, Gannon PJ, et al. Antiretroviral drugs induce oxidative stress and neuronal damage in the central nervous system. *J Neuro-Oncol*. 2014; 20:39–53.
- Anthonypillai C, Sanderson RN, Gibbs JE, Thomas SA. The distribution of the HIV protease inhibitor, ritonavir, to the brain, cerebrospinal fluid, and choroid plexuses of the Guinea pig. *J Pharmacol Exp Ther*. 2004; 308:912–920. [PubMed: 14634041]
- Baburamani AA, Ek CJ, Walker DW, Castillo-Melendez M. Vulnerability of the developing brain to hypoxic-ischemic damage: contribution of the cerebral vasculature to injury and repair? *Front Physiol*. 2012; 3:424. [PubMed: 23162470]
- Bertrand L, Nair M, Toborek M. Solving the blood-brain barrier challenge for the effective treatment of HIV replication in the central nervous system. *Curr Pharm Des*. 2016; 22:5477–5486. [PubMed: 27464720]
- Blas-Garcia A, Polo M, Alegre F, Funes HA, Martinez E, Apostolova N, Esplugues JV. Lack of mitochondrial toxicity of darunavir, raltegravir and rilpivirine in neurons and hepatocytes: a comparison with efavirenz. *J Antimicrob Chemother*. 2014; 69:2995–3000. [PubMed: 25011651]
- Borsa M, Ferreira PLC, Petry A, Ferreira LGE, Camargo MM, Bou-Habib DC, Pinto AR. HIV infection and antiretroviral therapy lead to unfolded protein response activation. *Virology*. 2015; 12:77. [PubMed: 25976933]

- Brown LA, Jin J, Ferrell D, Sadic E, Obregon D, Smith AJ, Tan J, Giunta B. Efavirenz promotes β -secretase expression and increased A β 1-40,42 via oxidative stress and reduced microglial phagocytosis: implications for HIV associated neurocognitive disorders (HAND). *PLoS One*. 2014; 9:1–9.
- Caniglia EC, Cain LE, Justice A, Tate J, Logan R, Sabin C, Winston A, et al. Antiretroviral penetration into the CNS and incidence of AIDS-defining neurologic conditions. *Neurology*. 2014; 83:134–141. [PubMed: 24907236]
- Capetti A, Cossu MV, Rizzardini G. Darunavir/cobicistat for the treatment of HIV-1: a new era for compact drugs with high genetic barrier to resistance. *Expert Opin Pharmacother*. 2015; 16:2689–2702. [PubMed: 26612518]
- Carvalho A, Gill MJ, Letendre SL, Rachlis A, Bekele T, Raboud J, Burchell A, Rourke SB, HIV/AIDS and the C. for B. H. Central nervous system penetration effectiveness of antiretroviral drugs and neuropsychological impairment in the Ontario HIV Treatment Network cohort study. *J Neuro-Oncol*. 2016; 22:349–357.
- Centers for Disease Control and Prevention. HIV Surveillance Report, 2015. 2016.
- Chen J. Heme oxygenase in neuroprotection: from mechanisms to therapeutic implications. *Rev Neurosci*. 2014; 25:269–280. [PubMed: 24501157]
- Chen MF, Gill AJ, Kolson DL. Neuropathogenesis of HIV-associated neurocognitive disorders. *Curr Opin HIV AIDS*. 2014; 9:559–564. [PubMed: 25203638]
- Cohen RA, Seider TR, Navia B. HIV effects on age-associated neurocognitive dysfunction: premature cognitive aging or neurodegenerative disease? *Alzheimers Res Ther*. 2015; 7:37. [PubMed: 25848401]
- Cottrell ML, Hadzic T, Kashuba ADM. Clinical pharmacokinetic, pharmacodynamic and drug-interaction profile of the integrase inhibitor dolutegravir. *Clin Pharmacokinet*. 2013; 52:981–994. [PubMed: 23824675]
- Cross SA, Cook DR, Chi AWS, Vance PJ, Kolson LL, Wong BJ, Jordan-Sciutto KL, Kolson DL. Dimethyl fumarate, an immune modulator and inducer of the antioxidant response, suppresses HIV replication and macrophage-mediated neurotoxicity: a novel candidate for HIV neuroprotection. *J Immunol*. 2011; 187:5015–5025. [PubMed: 21976775]
- de Boer MGJ, van den Berk GEL, van Holten N, Orszycyn JE, Dorama W, Moha DA, Brinkman K. Intolerance of dolutegravir-containing combination antiretroviral therapy regimens in real-life clinical practice. *AIDS*. 2016; 30:2831–2834. [PubMed: 27824625]
- de Gassart A, Bujisic B, Zaffalon L, Decosterd LA, di Micco A, Frera G, Tallant R, Martinon F. An inhibitor of HIV-1 protease modulates constitutive eIF2 α dephosphorylation to trigger a specific integrated stress response. *Proc Natl Acad Sci U S A*. 2016; 113:E117–E126. [PubMed: 26715744]
- Deeks ED. Darunavir: a review of its use in the management of HIV-1 infection. *Drugs*. 2014; 74:99–125. [PubMed: 24338166]
- Department of Health and Human Services (DHHS). Panel on Antiretroviral Guidelines for Adults and Adolescents. Guidelines for the use of antiretroviral agents in HIV-1-infected adults and adolescents. 2016a. Available at <http://www.aidsinfo.nih.gov/ContentFiles/AdultandAdolescentGL.pdf>. Accessed 22 August 2017
- Department of Health and Human Services (DHHS). Panel on Antiretroviral Therapy and Medical Management of HIV-Infected Children. Guidelines for the Use of Antiretroviral Agents in Pediatric HIV Infection. 2016b. Available at <http://aidsinfo.nih.gov/contentfiles/lvguidelines/pediatricguidelines.pdf>. Accessed 22 August 2017
- Gannon PJ, Akay-Espinoza C, Yee AC, Briand LA, Erickson MA, Gelman BB, Gao Y, et al. HIV protease inhibitors Alter amyloid precursor protein processing via β -site amyloid precursor protein cleaving enzyme-1 translational up-regulation. *Am J Pathol*. 2017; 187:91–109. [PubMed: 27993242]
- Gao X, Wang S, Yang X, Lan W, Chen Z, Chen J, Xie J, Han Y, Pi R, Yang X. Gartanin protects neurons against glutamate-induced cell death in HT22 cells: independence of Nrf-2 but involvement of HO-1 and AMPK. *Neurochem Res*. 2016; 41:2267–2277. [PubMed: 27161377]

- Gelman BB, Schuenke K. Brain aging in acquired immunodeficiency syndrome: increased ubiquitin-protein conjugate is correlated with decreased synaptic protein but not amyloid plaque accumulation. *J Neuro-Oncol.* 2004; 10:98–108.
- Grant I, Franklin DR, Deutsch R, Woods SP, Vaida F, Ellis RJ, Letendre SL, et al. Asymptomatic HIV-associated neurocognitive impairment increases risk for symptomatic decline. *Neurology.* 2014; 82:2055–2062. [PubMed: 24814848]
- Halliday M, Mallucci GR. Targeting the unfolded protein response in neurodegeneration: a new approach to therapy. *Neuropharmacology.* 2014; 76:169–174. [PubMed: 24035917]
- Halliday M, Radford H, Sekine Y, Moreno J, Verity N, le Quesne J, Ortori CA, et al. Partial restoration of protein synthesis rates by the small molecule ISRIB prevents neurodegeneration without pancreatic toxicity. *Cell Death Dis.* 2015; 6:e1672. [PubMed: 25741597]
- Hetz C, Mollereau B. Disturbance of endoplasmic reticulum proteostasis in neurodegenerative diseases. *Nat Rev Neurosci.* 2014; 15:233–249. [PubMed: 24619348]
- Hoffmann C, Welz T, Sabranski M, Kolb M, Wolf E, Stellbrink H-J, Wyen C. Higher rates of neuropsychiatric adverse events leading to dolutegravir discontinuation in women and older patients. *HIV Med.* 2017; 18:56–63. [PubMed: 27860104]
- Kanters S, Vitoria M, Doherty M, Socias ME, Ford N, Forrest JI, Popoff E, et al. Comparative efficacy and safety of first-line antiretroviral therapy for the treatment of HIV infection: a systematic review and network meta-analysis. *Lancet HIV.* 2016; 3:e510–e520. [PubMed: 27658869]
- Kaul M, Lipton SA. Mechanisms of Neuroimmunity and neurodegeneration associated with HIV-1 infection and AIDS. *J NeuroImmune Pharmacol.* 2006; 1:138–151. [PubMed: 18040780]
- Kheloufi F, Allemand J, Mokhtari S, Default A. Psychiatric disorders after starting dolutegravir. *AIDS.* 2015; 29:1723–1725. [PubMed: 26372287]
- Lai DJ, Tarwater PM, Hardy RJ. Measuring the impact of HIV/AIDS, heart disease and malignant neoplasms on life expectancy in the USA from 1987 to 2000. *Public Health.* 2006; 120:486–492. [PubMed: 16730037]
- Letendre SL, Mills AM, Tashima KT, Thomas DA, Min SS, Chen S, Song IH, Piscitelli SC, extended ING116070 study team. ING116070: a study of the pharmacokinetics and antiviral activity of Dolutegravir in cerebrospinal fluid in HIV-1-infected, antiretroviral therapy-naive subjects. *Clin Infect Dis.* 2014; 59:1032–1037. [PubMed: 24944232]
- Linden T, Doutheil J, Paschen W. Role of calcium in the activation of erp72 and heme oxygenase-1 expression on depletion of endoplasmic reticulum calcium stores in rat neuronal cell culture. *Neurosci Lett.* 1998; 247:103–106. [PubMed: 9655603]
- Lindl KA, Akay C, Wang Y, White MG, Jordan-Sciutto KL. Expression of the endoplasmic reticulum stress response marker, BiP, in the central nervous system of HIV-positive individuals. *Neuropathol Appl Neurobiol.* 2007; 33:658–669. [PubMed: 17931354]
- Lu M-C, Ji J-A, Jiang Z-Y, You Q-D. The Keap1-Nrf2-ARE pathway as a potential preventive and therapeutic target: an update. *Med Res Rev.* 2016; 36:924–963. [PubMed: 27192495]
- Marra CM, Zhao Y, Clifford DB, Letendre S, Evans S, Henry K, Ellis RJ, et al. Impact of combination antiretroviral therapy on cerebrospinal fluid HIV RNA and neurocognitive performance. *AIDS.* 2009; 23:1359–1366. [PubMed: 19424052]
- Mills AM, Nelson M, Jayaweera D, Ruxrungtham K, Cassetti I, Girard P-M, Workman C, et al. Once-daily darunavir/ritonavir vs. lopinavir/ritonavir in treatment-naive, HIV-1-infected patients: 96-week analysis. *AIDS.* 2009; 23:1679–1688. [PubMed: 19487905]
- Nakagawa S, Castro V, Toborek M. Infection of human pericytes by HIV-1 disrupts the integrity of the blood-brain barrier. *J Cell Mol Med.* 2012; 16:2950–2957. [PubMed: 22947176]
- Noguera-Julian A, Morén C, Rovira N, Garrabou G, Catalán M, Sánchez E, Cardellach F, Miró Ó, Fortuny C. Decreased mitochondrial function among healthy infants exposed to Antiretrovirals during gestation, delivery and the neonatal period. *Pediatr Infect Dis J.* 2015; 34:1349–1354. [PubMed: 26372453]
- Podany AT, Scarsi KK, Fletcher CV. Comparative clinical pharmacokinetics and pharmacodynamics of HIV-1 integrase strand transfer inhibitors. *Clin Pharmacokinet.* 2017; 56:25–40. [PubMed: 27317415]

- Ramanathan S, Mathias AA, German P, Kearney BP. Clinical pharmacokinetic and Pharmacodynamic profile of the HIV integrase inhibitor Elvitegravir. *Clin Pharmacokinet.* 2011; 50:229–244. [PubMed: 21348537]
- Robertson K, Liner J, Meeker RB. Antiretroviral neurotoxicity. *J Neuro-Oncol.* 2012; 18:388–399.
- Sacktor N, Skolasky RL, Seaberg E, Munro C, Becker JT, Martin E, Ragin A, Levine A, Miller E. Prevalence of HIV-associated neurocognitive disorders in the multicenter AIDS cohort study. *Neurology.* 2016; 86:334–340. [PubMed: 26718568]
- Saunders NR, Liddelow SA, Dziegielewska KM. Barrier mechanisms in the developing brain. *Front Pharmacol.* 2012; 3:46. [PubMed: 22479246]
- Saylor D, Dickens AM, Sacktor N, Haughey N, Slusher B, Pletnikov M, Mankowski JL, Brown A, Volsky DJ, McArthur JC. HIV-associated neurocognitive disorder–pathogenesis and prospects for treatment. *Nat Rev Neurol.* 2016; 12:234–248. [PubMed: 26965674]
- Schuller DJ, Poulos TL, Wilks A, de Montellano PO. Crystallization of recombinant human heme oxygenase-1. *Protein Sci.* 1998; 7:1836–1838. [PubMed: 10082382]
- Shah A, Gangwani MR, Chaudhari NS, Glazyrin A. Neurotoxicity in the post-HAART era: caution for the antiretroviral therapeutics. *Neurotox Res.* 2016; 30:677–697. [PubMed: 27364698]
- Sidrauski C, Acosta-Alvear D, Khoutorsky A, Vedantham P, Hearn BR, Li H, Gamache K, et al. Pharmacological brake-release of mRNA translation enhances cognitive memory. *elife.* 2013; 2:e00498. [PubMed: 23741617]
- Singh MV, Davidson DC, Jackson JW, Singh VB, Silva J, Ramirez SH, Maggirwar SB. Characterization of platelet–monocyte complexes in HIV-1–infected individuals: possible role in HIV-associated Neuroinflammation. *J Immunol.* 2014; 192:4674–4684. [PubMed: 24729609]
- Singh H, Kaur M, Kakkar AK, Kumar H. The promise of Dolutegravir: a novel second generation integrase strand transfer inhibitor. *Curr Clin Pharmacol.* 2016a; 11:88–94. [PubMed: 27157040]
- Singh VB, Singh MV, Gorantla S, Poluektova LY, Maggirwar SB, Heaton RK, McArthur JC, et al. Smoothed agonist reduces human immunodeficiency virus type-1-induced blood-brain barrier breakdown in humanized mice. *Sci Rep.* 2016b; 6:26876. [PubMed: 27241024]
- Smurzynski M, Wu K, Letendre S, Robertson K, Bosch RJ, Clifford DB, Evans S, Collier AC, Taylor M, Ellis R. Effects of central nervous system antiretroviral penetration on cognitive functioning in the ALLRT cohort. *AIDS.* 2011; 25:357–365. [PubMed: 21124201]
- Tan IL, Smith BR, Hammond E, Vornbrock-Roosa H, Creighton J, Selnes O, McArthur JC, Sacktor N. Older individuals with HIV infection have greater memory deficits than younger individuals. *J Neuro-Oncol.* 2013; 19:531–536.
- Teeraananchai S, Kerr S, Amin J, Ruxrungtham K, Law M. Life expectancy of HIV-positive people after starting combination antiretroviral therapy: a meta-analysis. *HIV Med.* 2016; 18:256–66. [PubMed: 27578404]
- Tiraboschi JM, Knobel H, Imaz A, Villar J, Ferrer E, Saumoy M, González A, et al. Cerebrospinal fluid and plasma lopinavir concentrations and viral response in virologically suppressed patients switching to lopinavir/ritonavir monotherapy once daily. *Antivir Ther.* 2015; 21:359–363. [PubMed: 26656921]
- Treisman GJ, Soudry O. Neuropsychiatric effects of HIV antiviral medications. *Drug Saf.* 2016; 39:945–957. [PubMed: 27534750]
- Troya J, Bascuñana J. Safety and tolerability: current challenges to antiretroviral therapy for the long-term management of HIV infection. *AIDS Rev.* 2016; 18:127–137. [PubMed: 27651173]
- UNAIDS. AIDS by the numbers. 2015. Available at http://www.unaids.org/sites/default/files/media_asset/AIDS_by_the_numbers_2015_en.pdf. Accessed 22 Aug 2017
- Watson RE, Desesso JM, Hurtt ME, Cappon GD. Postnatal growth and morphological development of the brain: a species comparison. *Birth Defects Res Part B Dev Reprod Toxicol.* 2006; 77:471–484.
- Weiß M, Kost B, Renner-Müller I, Wolf E, Mylonas I, Brüning A. Efavirenz causes oxidative stress, endoplasmic reticulum stress, and autophagy in endothelial cells. *Cardiovasc Toxicol.* 2016; 16:90–99. [PubMed: 25666561]
- Wensing AMJ, van Maarseveen NM, Nijhuis M. Fifteen years of HIV protease inhibitors: raising the barrier to resistance. *Antiviral Res.* 2010; 85:59–74. [PubMed: 19853627]

- World Health Organization (WHO). Consolidated guidelines on the use of antiretroviral drugs for treating and preventing HIV infection: recommendations for a public health approach. 2016a. Available at http://apps.who.int/iris/bitstream/10665/208825/1/9789241549684_eng.pdf. Accessed 22 Aug 2017
- World Health Organization (WHO). Progress report 2016. Prevent HIV, test and treat all Prog Rep 2016 Prev HIV, Test Treat All. 2016b
- Wilcox KS, Buchhalter J, Dichter MA. Properties of inhibitory and excitatory synapses between hippocampal neurons in very low density cultures. *Synapse*. 1994; 18:128–151. [PubMed: 7839312]
- Yates MS, Tauchi M, Katsuoka F, Flanders KC, Liby KT, Honda T, Gribble GW, et al. Pharmacodynamic characterization of chemopreventive triterpenoids as exceptionally potent inducers of Nrf2-regulated genes. *Mol Cancer Ther*. 2007; 6:154–162. [PubMed: 17237276]
- Yilmaz A, Gisslén M, Spudich S, Lee E, Jayewardene A, Aweeka F, Price RW. Raltegravir cerebrospinal fluid concentrations in HIV-1 infection. *PLoS One*. 2009a; 4:e6877. [PubMed: 19721718]
- Yilmaz A, Izadkhashti A, Price RW, Mallon PW, de Meulder M, Timmerman P, Gisslén M. Darunavir concentrations in cerebrospinal fluid and blood in HIV-1–infected individuals. *AIDS Res Hum Retrovir*. 2009b; 25:457–461. [PubMed: 19320601]

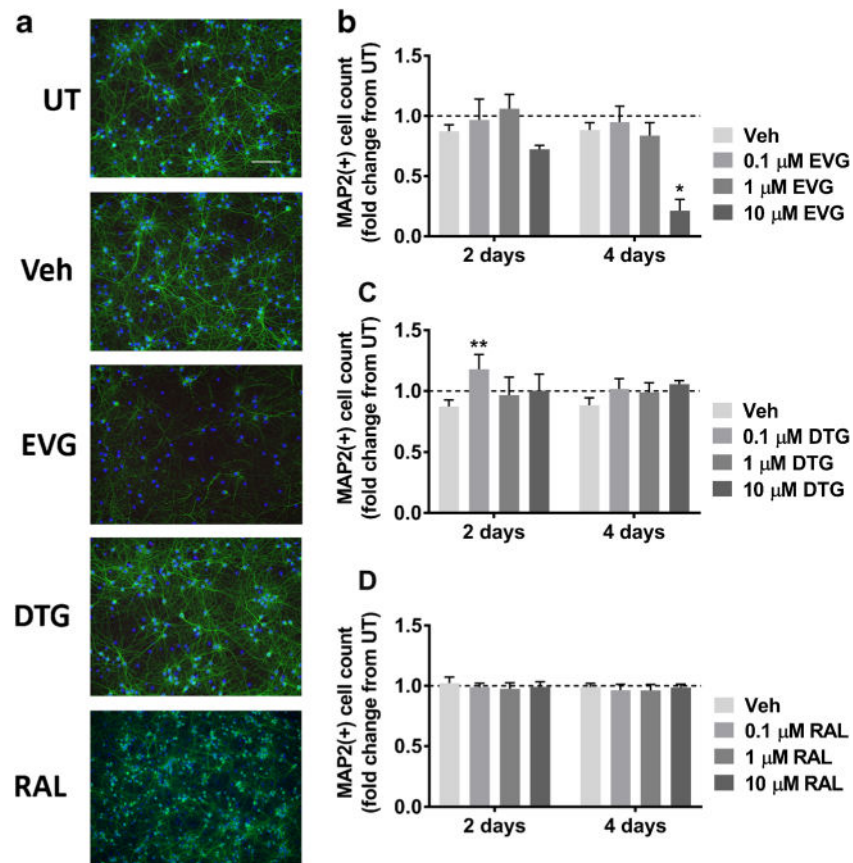


Fig. 1.

EVG but not DTG or RAL is toxic to primary rat cortical neuroglial cultures. **a** Cultures were treated with DMSO vehicle or 0.1 μ M, 1 μ M, or 10 μ M EVG, DTG, or RAL for either 2 days or every other day for 4 days. Representative images of neuroglial cultures immunostained for MAP2 (green) and DAPI (blue) after treatment with 10 μ M of indicated compounds for 4 days are shown at 20 \times magnification. Scale bar represents 100 μ M. **b-d** Quantification of MAP2+ cells treated with indicated compounds is shown (repeated measures two-way ANOVA followed by Dunnett's test, $n = 3$, * $p < 0.05$, ** $p < 0.01$ vs drug vehicle). Dashed lines represent untreated (UT) cultures

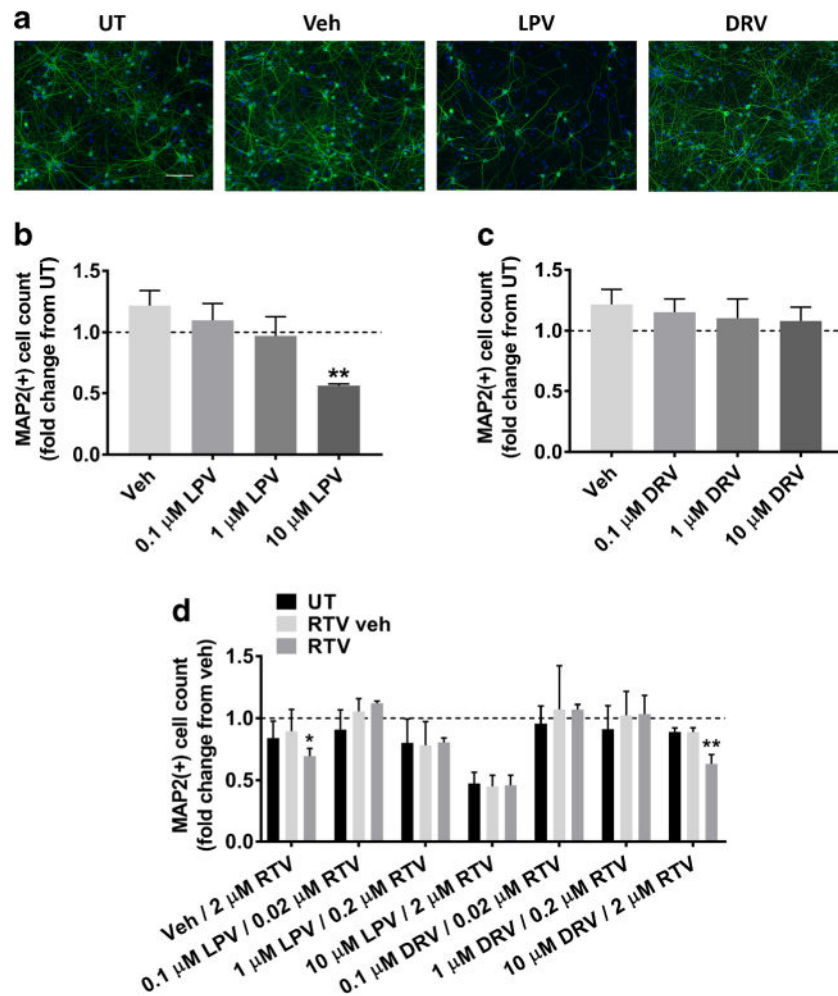


Fig. 2.

LPV but not DRV is toxic to primary rat cortical neuroglial cultures. **a** Cultures were treated with DMSO vehicle or 0.1 μM, 1 μM, or 10 μM LPV or DRV for 2 days. Representative images of neuroglial cultures immunostained for MAP2 (green) and DAPI (blue) after treatment with 10 μM of the indicated compounds are shown at 20× magnification. Scale bar represents 100 μM. **b–c** Quantification of MAP2+ cells treated with indicated compounds is shown (repeated measures one-way ANOVA followed by Dunnett's test, $n = 3$, $**p < 0.01$ vs drug vehicle). Dashed lines represent untreated (UT) cultures. **d** Neurons were treated with LPV and DRV with or without simultaneous RTV or RTV vehicle treatment. RTV booster concentrations were given in fixed ratios with LPV and DRV concentrations. Quantification of MAP2+ cells treated with indicated compounds is shown (repeated measures two-way ANOVA followed by Dunnett's test, $n = 3$, $*p < 0.05$, $**p < 0.01$ vs drug vehicle). Dashed line represents untreated (UT) cultures

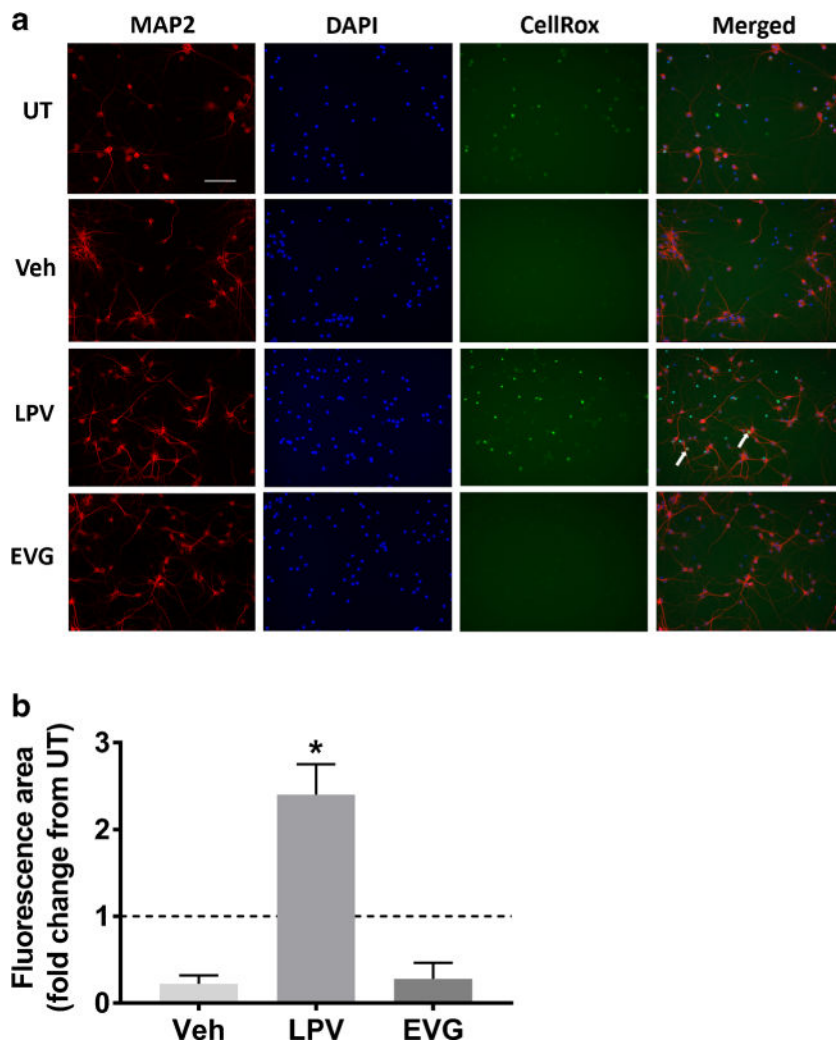


Fig. 3. LPV but not EVG induces oxidative stress. **a** Rat cortical neuroglial cultures were treated with DMSO vehicle or 10 μ M LPV or EVG for 1 h prior to the addition of CellRox Green reagent and live cell imaging. Images captured by time-lapse live imaging were merged with the images of the same cells that were subsequently fixed and immunostained for MAP2 and DAPI. Representative images captured 30 min following CellRox addition show cells immunostained for MAP2 (red), DAPI (blue), and CellRox green at 20 \times magnification. Scale bar represents 100 μ m; white arrows indicate examples of neurons that accumulated CellRox green dye. **b** Quantification of the area positive for CellRox green fluorescence normalized to untreated (UT) cultures (dashed line) is shown (repeated measures one-way ANOVA followed by Dunnett's test, $n = 4$, $*p < 0.05$ vs drug vehicle)

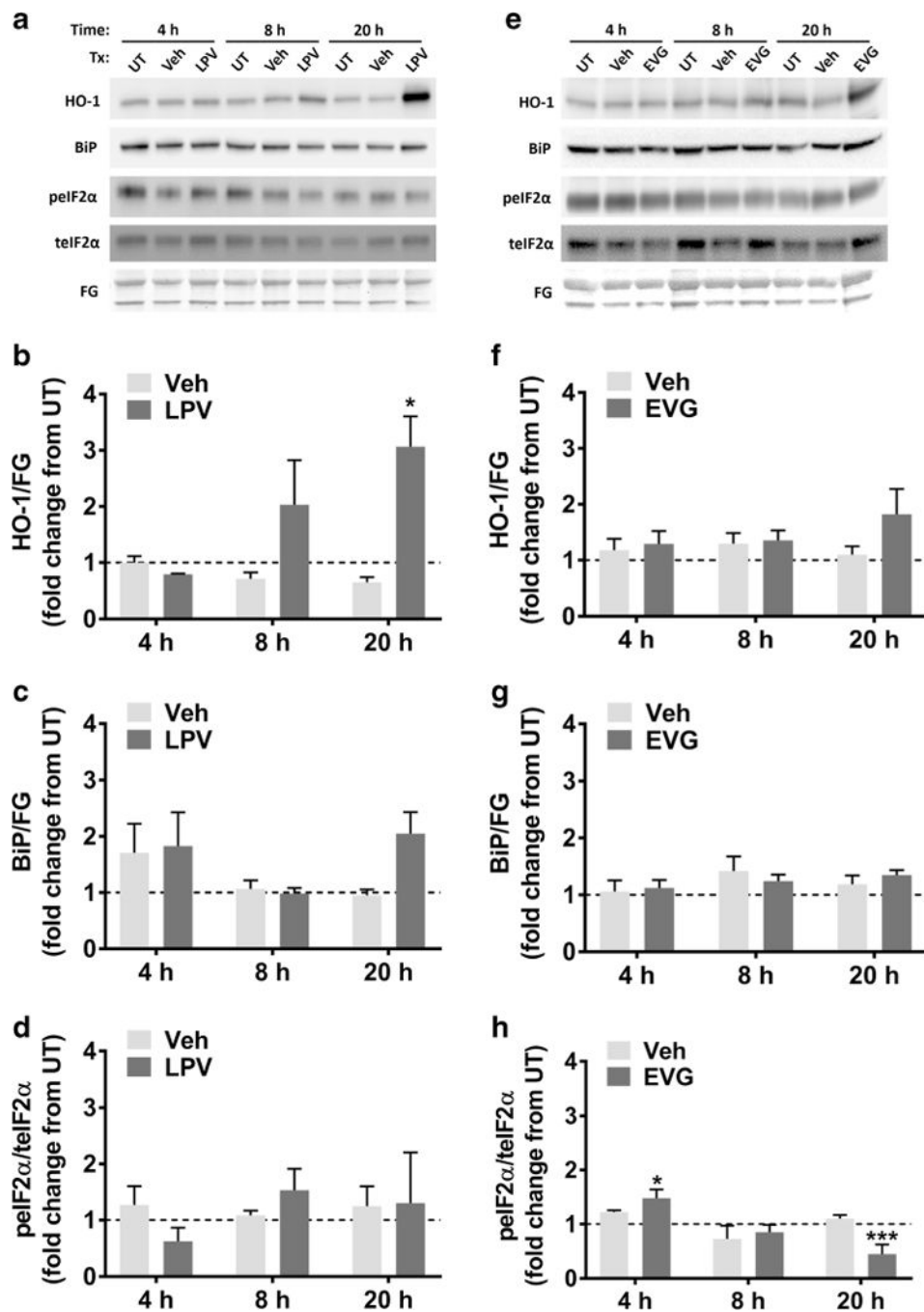


Fig. 4. LPV but not EVG induces the endogenous antioxidant response, while EVG but not LPV transiently increases the ratio of peIF2 α /telIF2 α . **a** Rat cortical neuroglial cultures were treated with DMSO vehicle or 10 μ M LPV for 4, 8, or 20 h. Representative blots are shown. FG, fast green loading control. **b–d** Band intensities of HO-1, BiP, peIF2 α , and telIF2 α were quantified using ImageJ software. HO-1 and BiP are normalized to FG, and peIF2 α is normalized to telIF2 α (repeated measures two-way ANOVA followed by Dunnett's test, $n = 3$, * $p < 0.05$ vs drug vehicle). Dashed lines represent untreated (UT) cultures. **e** Rat cortical

neuroglial cultures were treated with DMSO vehicle or 10 μ M EVG for 4, 8, or 20 h. Representative immunoblots are shown. FG, fast green loading control. **f–h** Band intensities of HO-1, BiP, peIF2 α , and teIF2 α were quantified using ImageJ software. HO-1 and BiP are normalized to FG, and peIF2 α is normalized to teIF2 α (repeated measures two-way ANOVA followed by Dunnett's test, $n = 3$, * $p < 0.05$, *** $p < 0.001$ vs drug vehicle). Dashed lines represent untreated (UT) cultures

Author Manuscript

Author Manuscript

Author Manuscript

Author Manuscript

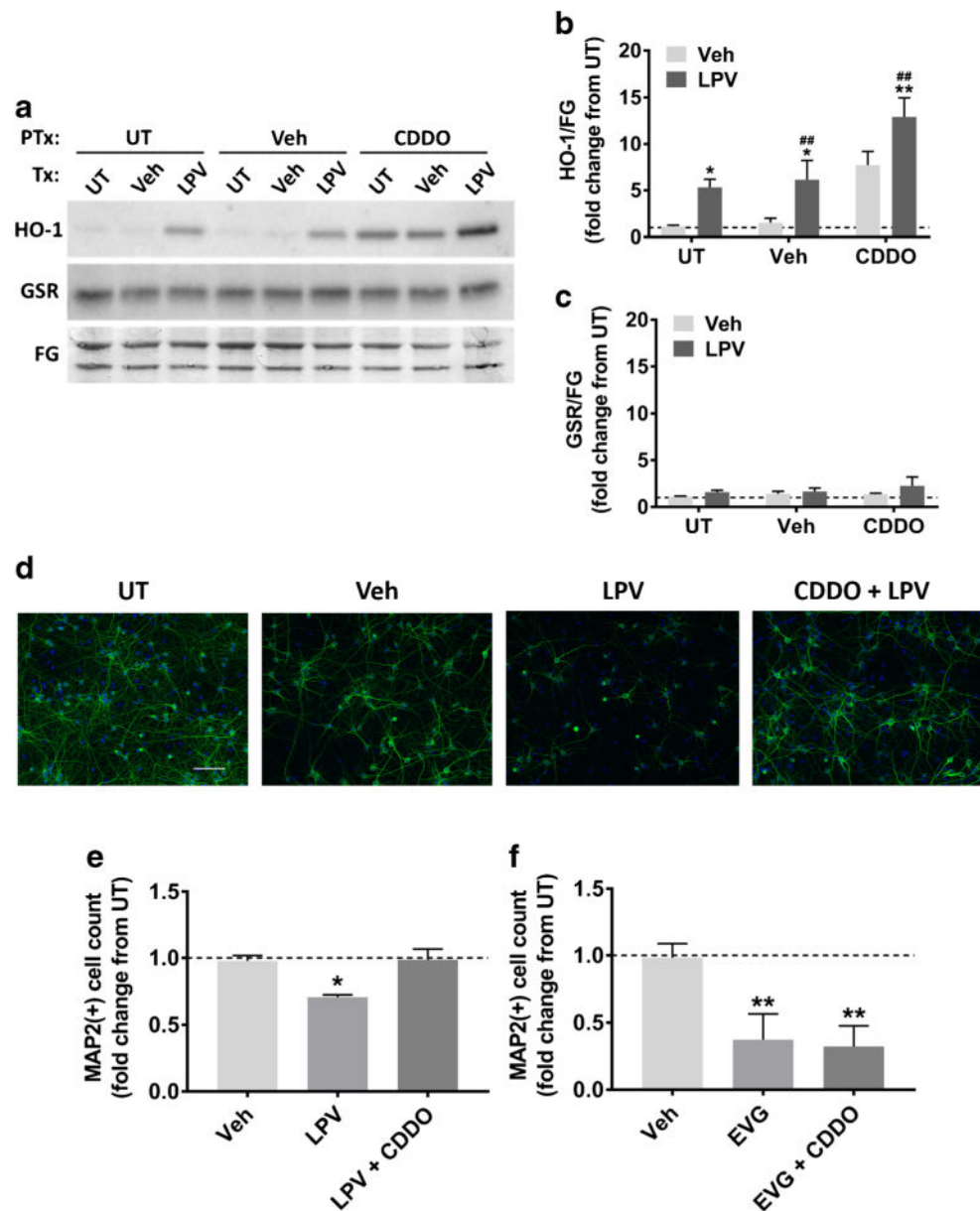


Fig. 5. Pharmacological induction of HO-1 is protective against LPV-induced neurotoxicity. **a** Rat cortical neuroglial cultures were pretreated with either DMSO vehicle or 0.1 μ M CDDO for 1 h prior to 20 h treatment with DMSO vehicle or 10 μ M LPV. Representative immunoblots are shown. GSR, glutathione reductase; FG, fast green loading control. **b–c** HO-1 and GSR band intensities were quantified using ImageJ software (repeated measures two-way ANOVA followed by Dunnett's test, $n = 3$, $*p < 0.05$, $**p < 0.01$ vs drug vehicle, $###p < 0.01$ vs CDDO vehicle). **d** Cultures were pretreated with either DMSO vehicle or 0.1 μ M CDDO for 1 h prior to 48 h treatment with DMSO vehicle or 10 μ M LPV. Representative images of LPV-treated cells immunostained for MAP2 (green) and DAPI (blue) are shown at 20 \times magnification. Scale bar represents 100 μ M. **e** Quantification of MAP2+ cells treated with indicated compounds is shown (repeated measures one-way ANOVA followed by Dunnett's

test, $n = 3$, $*p < 0.05$ vs drug vehicle). **f** Cultures were pretreated with DMSO vehicle or 0.1 μM CDDO for 1 h prior to 10 μM EVG treatment. After 48 h, cells were retreated with DMSO vehicle or 10 μM EVG for another 48 h, followed by immunostaining. Quantification of MAP2+ cells treated with indicated compounds is shown (repeated measures one-way ANOVA followed by Dunnett's test, $n = 3$, $**p < 0.01$ vs drug vehicle)

Author Manuscript

Author Manuscript

Author Manuscript

Author Manuscript

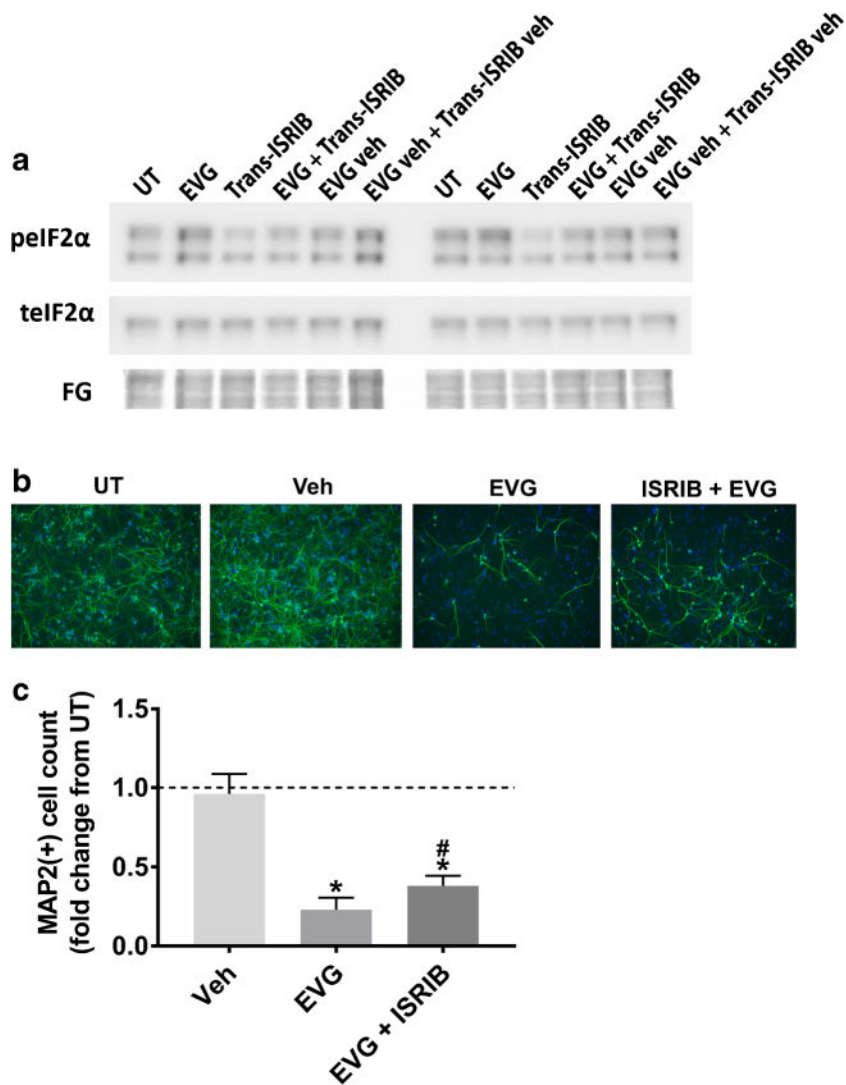


Fig. 6. Pharmacological inhibition of peIF2 α is partially protective against EVG-induced neurotoxicity. **a** Rat cortical neuroglial cultures were pretreated with DMSO vehicle or 5 μ M trans-ISRIB for 1 h before treatment with 10 μ M EVG for 4 h. Blots from two biological replicates are shown. FG, fast green loading control. **b** Rat cortical neuroglial cultures were pretreated with either DMSO vehicle or 5 μ M trans-ISRIB for 1 h prior to treatment with 10 μ M EVG every other day for 4 days. Representative images of neuroglial cultures immunostained for MAP2 (green) and DAPI (blue) after treatment with the indicated compounds for 4 days are shown at 20 \times magnification. Scale bar represents 100 μ M. **c** Quantification of MAP2+ cells treated with indicated compounds is shown (repeated measures two-way ANOVA followed by Dunnett's test, $n = 3$, * $p < 0.05$ vs drug vehicle, # $p < 0.05$ vs ISRIB vehicle). Dashed lines represent untreated (UT) cultures

Table 1

Reported patient plasma and cerebrospinal fluid concentrations of the antiretroviral drugs evaluated in this study. Concentration range is provided in ng/ml and the maximum measured concentration is provided in μM to allow for direct comparison with doses tested in the current study

Drug	Plasma concentration (ng/ml)	Maximum plasma concentration (μM)	CSF concentration (ng/ml)	Maximum CSF concentration (μM)
Elvitegravir ^a	450–1700	3.8	2.4–11.7	0.03
Dolutegravir ^b	220–3340	8.0	12.6–16.2	0.04
Raltegravir ^c	1140–1502	3.4	6.0–94.2	0.21
Lopinavir ^d	154–16,700	26.6	1.93–78.3	0.12
Darunavir ^e	1800–12,900	23.6	15.9–212	0.39

CSF Cerebrospinal fluid

^a(Ramanathan et al. 2011; Podany et al. 2017)

^b(Cottrell et al. 2013)

^c(Yilmaz et al. 2009a)

^d(Tiraboschi et al. 2015)

^e(Yilmaz et al. 2009b)